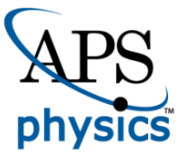

Nonlocal energy-optimized kernel: Recovering second-order exchange in the homogeneous electron gas

Jefferson E. Bates, Savio Laricchia, and Adrienn Ruzsinszky

Phys. Rev. B **93**, 045119 — Published 19 January 2016

DOI: 10.1103/PhysRevB.93.045119

A Non-Local, Energy-Optimized Kernel: Recovering Second-Order Exchange in the Homogeneous Electron Gas

Jefferson E. Bates,* Savio Laricchia,† and Adrienn Ruzsinszky
Department of Physics, Temple University, Philadelphia, Pennsylvania 19122, United States

In order to remedy some of the shortcomings of the Random Phase Approximation (RPA) within Adiabatic Connection Fluctuation-Dissipation (ACFD) Density Functional Theory we introduce a short-ranged, exchange-like kernel that is one-electron self-correlation free and exact for two-electron systems in the high density limit. By tuning a free parameter in our model to recover an exact limit of the homogeneous electron gas correlation energy we obtain a non-local, energy-optimized kernel that reduces the errors of RPA for both homogeneous and inhomogeneous solids. Using wave-vector symmetrization for the kernel, we also implement RPA renormalized perturbation theory for extended systems, and demonstrate its capability to describe the dominant correlation effects with a low-order expansion in both metallic and non-metallic systems. The comparison of ACFD structural properties with experiment is also shown to be limited by the choice of norm conserving pseudopotential.

I. INTRODUCTION

Local and semi-local density functional theory[1–5] is an efficient and useful tool for studying the electronic structure of molecules and materials. Its accuracy is limited, however, and has not reached the accuracy criteria of the chemical and semiconductor industries. Famous failures of semi-local density functional theory (DFT) include self-interaction errors[6,7], the absence of long-range van der Waals interactions[8], and the missing derivative discontinuity[9] with respect to changes in particle number. New methods must therefore be developed that overcome the known problems of standard functionals, without drastically increasing the computational cost. There has been a growing interest in the direct random phase approximation (RPA) as a possible solution to many of these problems.[10–12] RPA stands on the fifth and highest rung of Jacob's ladder[13] of density functional approximations, employing the unoccupied as well as the occupied Kohn-Sham orbitals in a fully non-local way. Since the RPA energy includes the exact-exchange energy, self-interaction error is greatly reduced, and the correlation contribution naturally includes long-range van der Waals interactions.[14–19]

Nevertheless, direct RPA is limited by the neglect of short-ranged correlation described by an exchange-correlation (xc) kernel within the adiabatic-connection fluctuation-dissipation (ACFD) DFT framework[20]. The lack of a proper description of the short-ranged correlation within RPA results in inaccurate total, ionization, atomization and cohesive energies[21–23], and in certain inaccurate structural phase transition pressures[24]. Even though the RPA short-ranged correlation is actually an overestimate[25,26], this error largely cancels out of energy differences at constant electron number[22], but less so for energy differences that change the number of electron-pairs.[12,20,26,27] While kernels such as the exact-exchange (EXX) kernel[28,29] provide greatly improved accuracy for total energies they simultaneously degrade the computational efficiency of RPA making their broad applicability a challenge. Electron gas model kernels[30–33] have recently been tested for applications in inhomogeneous systems, showing some moderate improvements over RPA[34,35].

Here we propose a non-local, energy-optimized[36] (NEO) meta-generalized gradient approximation (MGGA) xc kernel in order to address some of the challenges facing semi-local DFT. This kernel contains one free parameter that can be used to modify its range, but remains one-electron self-correlation free and exact for two-electron systems in the high density limit regardless of this freedom. We test the behavior of the NEO kernel with variations in this parameter, and determine a constraint on its value from the second-order exchange energy of the uniform electron gas.

In addition to the choice of the kernel, the approach used to compute the interacting density-density response function, $\chi(\mathbf{r}, \mathbf{r}'; \omega)$, as well as the choice of reference determinant and pseudopotential play an important role in determining the overall performance of an ACFD-DFT approach. For a given reference, the traditional ACFD method solves the Dyson-like equation for the response function by inversion of an effective dielectric matrix which can become unstable even for kernels such as EXX in systems as simple as the electron gas or stretched diatomics.[29] Low-order perturbation theories avoid the instability, but are not broadly applicable due to divergences for zero-gap systems such as metals.[37] A renormalization approach based on RPA has been reported[38] that suggests a low-order expansion of the Dyson equation in powers of the RPA response function remains finite for small-gap systems, is sufficiently accurate, and also avoids instabilities. This approach allows for a natural decomposition of the correlation energy into RPA and beyond-RPA contributions, facilitating the analysis of the kernel's behavior in combination with different approximate response functions.

We also find that choosing an LDA or GGA norm-conserving pseudopotential makes the largest impact in the comparison of ACFD structural results to experi-

ment, but that the impact of correlation is analogous for both references. We explore the behavior of RPA renormalization below for both homogeneous and inhomegenous systems, as well as the impact of the reference pseudopotential.

II. ADIABATIC CONNECTION FLUCTUATION-DISSIPATION DFT AND THE NEO KERNEL

Within the ACFD framework, the exact correlation energy can be expressed as

$$E_{\rm c} = -\frac{1}{2\pi}\int d\mathbf{r}\, d\mathbf{r}'\, V(\mathbf{r},\mathbf{r}') \times \int_0^\infty d\omega \int_0^1 d\lambda\, {\rm Im}\left[\chi_\lambda(\mathbf{r},\mathbf{r}';\omega) - \chi_0(\mathbf{r},\mathbf{r}';\omega)\right], \tag{1}$$

where $V(\mathbf{r},\mathbf{r}') = 1/|\mathbf{r}-\mathbf{r}'|$ is the Coulomb interaction, Im indicates the imaginary part and atomic units are used unless otherwise specified. The total energy is computed as $E = E^{\rm EXX} + E_c$, where $E^{\rm EXX}$ is the Hartree-Fock exact-exchange energy evaluated using KS orbitals. The density-density response functions χ_λ and χ_0 satisfy the Dyson-like equation

$$\chi_\lambda(\mathbf{r},\mathbf{r}';\omega) = \chi_0(\mathbf{r},\mathbf{r}';\omega) + \int d\mathbf{r}_1 d\mathbf{r}_2\, \chi_0(\mathbf{r},\mathbf{r}_1;\omega) \times \left[V_\lambda(\mathbf{r}_1,\mathbf{r}_2) + f_{\rm xc}^\lambda(\mathbf{r}_1,\mathbf{r}_2;\omega)\right]\chi_\lambda(\mathbf{r}_2,\mathbf{r}';\omega), \tag{2}$$

where $\chi_0(\omega)$ is the Kohn-Sham (KS) response function, and $f_{\rm xc}(\omega)$ is the exact, frequency-dependent exchange-correlation (xc) kernel.[39] The coupling-strength dependence of the Coulomb interaction is $V_\lambda = \lambda V$, and that of $f_{\rm xc}^\lambda$ can be deduced from uniform coordinate scaling, Eqs. (17) and (18) in Ref 40. Once the kernel and the KS response function have been specified, the interacting response function can be obtained from Eq. (2) and the correlation energy computed from Eq. (1).

Under periodic boundary conditions, the Fourier transform of Eq. (1) can be represented as a sum of weighted contributions from wave-vectors $\mathbf{q}$ inside the first Brillouin zone

$$E_{\rm c} = -\frac{1}{2\pi}\sum_{\mathbf{q}}\int_0^\infty du \int_0^1 d\lambda \times {\rm Re}\,\left\langle V(\mathbf{q})\left[\chi_\lambda(\mathbf{q};iu) - \chi_0(\mathbf{q};iu)\right]\right\rangle, \tag{3}$$

where $\langle A\rangle$ indicates the trace of matrix A, the two-point functions V and χ are now replaced by two-index matrices in the reciprocal lattice vector basis, and the frequency integration has been changed to the imaginary axis ($\omega \to iu$, Im $\to$ Re). For uniform systems, only the "head" ($\mathbf{G} = \mathbf{G}' = 0$) of these matrices is required and after some algebra the correlation energy per electron reduces to[40]

$$\epsilon_c = -\frac{1}{\pi^2 n}\int_0^\infty dq \int_0^\infty du \int_0^1 d\lambda \times \chi_0(q;iu)\left[V_\lambda(q) + f_{\rm xc}^\lambda(q;iu)\right]\chi_\lambda(q;iu), \tag{4}$$

where $\chi_0(q;iu)$ is the Lindhard function. The choice $f_{\rm xc}^\lambda = 0$ with $\chi_\lambda = \hat{\chi}_\lambda = (1-\chi_0 V_\lambda)^{-1}\chi_0$ defines the RPA response function and correlation energy[11]

$$E_c^{\rm RPA} = \frac{1}{2\pi}\sum_{\mathbf{q}}\int_0^\infty du \times \left\langle \ln\left[1-\chi_0(\mathbf{q};iu)V(\mathbf{q})\right] + \chi_0(\mathbf{q};iu)V(\mathbf{q})\right\rangle. \tag{5}$$

Going beyond RPA, our NEO kernel approximation has the following non-local[40], but short-ranged form for a homogeneous system

$$f_{\rm x}^{\rm NEO}[n,z](\mathbf{r},\mathbf{r}') = -V(\mathbf{r},\mathbf{r}')\sum_\sigma\left(\frac{n_\sigma}{n}\right)^2 \times {\rm erfc}\left(|\mathbf{r}-\mathbf{r}'|\sqrt{\tilde{c}(1-z_\sigma^2)k_{F\sigma}^2}\right), \tag{6}$$

where erfc is the complementary error function, n_σ and n are the σ-spin and total density, respectively, $z_\sigma = \tau_\sigma^W/\tau_\sigma$ is a common meta-GGA ingredient[41,42], $\tau_\sigma^W = |\nabla n_\sigma|^2/(8n_\sigma)$ is the von Weizsäcker kinetic energy density, and τ_σ is the Kohn-Sham kinetic energy density

$$\tau_\sigma(\mathbf{r}) = \frac{1}{2}\sum_j^{\rm occ}|\nabla\phi_{j\sigma}(\mathbf{r})|^2. \tag{7}$$

The overall coupling-strength dependence is exchange-like such that $f_{\rm x}^{\lambda,{\rm NEO}} = \lambda f_{\rm x}^{\rm NEO}$.

By construction this kernel yields correlation energies that are one-electron self-correlation free for $z_\sigma = 1$. In this limit erfc(0) = 1, thus for one-electron densities ($n_\uparrow = n; n_\downarrow = 0$) $f_{\rm x}^{\rm NEO}[n_\uparrow, 1] = -V$. For two electrons in a spin-singlet ($n_\uparrow = n_\downarrow = n/2$) $f_{\rm x}^{\rm NEO}[2n_\uparrow, 1] = -V/2$, recovering the EXX kernel, which is exact in the high-density limit. For a uniform system, the Fourier transform of Eq. (6) to momentum space is also analytic resulting in

$$f_{\rm x}^{\rm NEO}[n,z](q) = -\frac{4\pi}{q^2}\sum_\sigma\left(\frac{n_\sigma}{n}\right)^2 \times\left(1-\exp\left(-\frac{q^2}{4\tilde{c}(1-z_\sigma^2)k_{F\sigma}^2}\right)\right). \tag{8}$$

Instead of satisfying known constraints of the xc kernel for the q and ω behavior for the electron gas, we follow the energy-optimization idea of Dobson and Wang[36], and Jung *et al.*[43] Similarly to the kernel of Ref. 43 and in contrast to the purely local form used by Dobson and Wang,

the NEO kernel is of short, but non-zero range. We intentionally substitute the complicated momentum and frequency dependence of the xc kernel with a parameter that can be tied to an integrated property such as the correlation energy. The NEO kernel tends to a constant as $q \to 0$, however, and will therefore approximately satisfy the exact, adiabatic LDA exchange limit for the electron gas kernel[31,35], but we do not expect to satisfy any other known constraints on the momentum and frequency dependence of $f_{\rm xc}$. Instead the $\tilde{c}$ parameter in NEO can be used to uniquely fit the exact second-order exchange contribution to the correlation energy for the electron gas, which is known analytically for all spin polarizations[44], $\epsilon_c^{(2,x)} = 0.02418$ a.u. Therefore we have the constraint that

$$\epsilon_c^{(2,x)}[f_{\rm x}^{\rm NEO}] = -\frac{1}{2\pi^2 n}\int_0^\infty dq \int_0^\infty du \times \chi_0(q;iu) f_{\rm x}^{\rm NEO}(q) \chi_0(q;iu)\,, \quad (9)$$

must equal the analytic result. Since $\tilde{c}$ determines $f_{\rm x}^{\rm NEO}$ and the kernel determines $\epsilon_c^{(2,x)}$, we can find a value of $\tilde{c}$ that satisfies this constraint for a given spin-polarization. Using the expressions given in the literature[45,46] to evaluate the RPA and beyond RPA correlation energy, the value $\tilde{c} = 0.264$ results in $\epsilon_c^{(2,x)}[f_{\rm x}^{\rm NEO}] = 0.02418$ a.u. for both the fully spin-polarized and unpolarized electron gas; for intermediate spin polarizations the error is less than 1.5 mH. In Sec. V we explore the behavior of NEO with respect to changes in $\tilde{c}$ to determine if this constraint produces a useful value of the parameter.

III. RPA RENORMALIZATION

Together with the kernel, the method used to determine the response function defines an ACFD approach. Ref 38 suggested that rather than using a non-interacting reference to compute the interacting response function as (suppressing momentum and frequency dependence)

$$\chi_\lambda = \left[1 - \chi_0\left(V_\lambda + f_{\rm xc}^\lambda\right)\right]^{-1}\chi_0\,, \quad (10)$$

the RPA response function could be used directly instead. Within such a framework, the density-density response function can be exactly reformulated as

$$\chi_\lambda = (1 - \hat{\chi}_\lambda f_{\rm xc}^\lambda)^{-1}\hat{\chi}_\lambda = \hat{\chi}_\lambda + \hat{\chi}_\lambda f_{\rm xc}^\lambda \chi_\lambda\,, \quad (11)$$

where $f_{\rm xc}^\lambda$ is the exact, frequency-dependent exchange-correlation (xc) kernel and $\hat{\chi}_\lambda$ is the RPA response function.

If Eq. (11) is expanded in powers of $\hat{\chi}_\lambda f_{\rm xc}^\lambda$ this approach avoids divergences of single-reference perturbation theory due to small non-interacting gaps, as well as those from instabilities in the response function, and does not significantly increase the computational cost in comparison to RPA[29,38]. Below we show that the first-order approximation recovers the dominant contributions of the infinite-order method, Eq. (10). Using Eqs. (11) and (1), the exact correlation energy can be decomposed into the RPA contribution plus a beyond-RPA (bRPA) correction that is a functional of the kernel, $E_c = E_c^{\rm RPA} + \Delta E_c^{\rm bRPA}[f_{\rm xc}]$, where

$$\Delta E_c^{\rm bRPA}[f_{\rm xc}] = -\frac{1}{2\pi}\sum_{\mathbf{q}}\int_0^\infty du \int_0^1 d\lambda \times \left\langle V(\mathbf{q})\hat{\chi}_\lambda(\mathbf{q};iu) f_{\rm xc}^\lambda(\mathbf{q};iu)\chi_\lambda(\mathbf{q};iu)\right\rangle. \quad (12)$$

While this expression requires more work than the original ACFD formulation in Eq. (1) because both $\hat{\chi}_\lambda$ and χ_λ must be computed, we can approximate χ_λ in order to reduce the cost to roughly that of RPA when using exchange-like kernels.

Rather than compute the infinite-order response function in Eq. (12), RPA renormalization effectively replaces it with a lower order approximation. The expansion of Eq. (11) to linear-order in $f_{\rm xc}$ defines RPA renormalized perturbation theory to first-order (RPAr1)

$$\chi_\lambda^{\rm RPAr1} = \hat{\chi}_\lambda + \hat{\chi}_\lambda f_{\rm xc}^\lambda \hat{\chi}_\lambda\,. \quad (13)$$

This approach proved to be an accurate and robust approximation when combined with an approximate exchange kernel (AXK), producing a systematic correction to RPA for ionization, atomization, barrier heights, and reaction energies.[38] While the method discussed in Ref. 38 was called AXK, this name referred to the combination of RPAr1 with a particular kernel. Likewise in Ref. 29, the combination of the EXX kernel with RPAr1 was called t'RPAx. Instead of creating a new name, we append the kernel name to RPAr1 to indicate which kernel is being used in Eq. (13).

Another alternative approximation to the infinite-order method is obtained by replacing one of the $\hat{\chi}_\lambda$ with χ_0 in Eq. (13)

$$\tilde{\chi}_\lambda = \hat{\chi}_\lambda + \chi_0 f_{\rm xc}^\lambda \hat{\chi}_\lambda\,. \quad (14)$$

Using the approximate exchange kernel suggested in Ref 38 with such a response function is equivalent to ACSOSEX[47], a method that is also one-electron self-correlation free. The original ACSOSEX is more or less equivalent to the SOSEX[48,49] correction proposed within a coupled cluster formalism. We will refer to Eq. (14) as ACSOSEX to avoid creating new terminology, and because the form of the resulting pair-density is equivalent to the original method. Both RPAr1 and ACSOSEX yield the exact second-order, unscreened perturbative correlation energy when the exact first-order kernel is used, but differ in their higher-order contributions.[38,47] Below we demonstrate that these two approximations behave systematically leading to an underestimation and overestimation, respectively, of the infinte-order bRPA correction. This trend is a direct consequence of replacing χ_λ in Eq. (12) with $\hat{\chi}_\lambda$ or χ_0.

IV. IMPLEMENTATION FOR INHOMOGENEOUS SYSTEMS

While the exact xc-kernel is naturally symmetric with respect to the interchange of $\mathbf{r}$ and $\mathbf{r}'$, model kernels are generally not and must be explicitly symmetrized. For an implementation in inhomogeneous systems using Gaussian basis sets these problems do not arise because one can work in terms of $|\mathbf{r}-\mathbf{r}'|$ and evaluate each of the densities in Eq. (6) at the electronic center of mass, $\mathbf{R}=(\mathbf{r}+\mathbf{r}')/2$, to preserve the symmetry.[50] For periodic boundary conditions, however, the kernel-symmetrization approach determines the spatial dependence of the densities.[34,35,51,52]

Recently Patrick and Thygesen[35] discussed the behavior of several variants of symmetrization, highlighting for each method the behavior of the "wings" (matrix elements with $\mathbf{G}\neq\mathbf{G}'=0$) in the limit $q\to 0$ for different kernels. The correct behavior of this limit is different for metallic[53] and non-metallic systems[54]. We have implemented the wave-vector symmetrization approach to extend our model kernel to inhomogeneous systems because it is more efficient than other real-space approaches, requiring integration only over the unit-cell and not the entire crystal volume.[35] Furthermore structural properties obtained with the wave-vector symmetrization exhibited smaller errors with respect to experiment compared to the two-point density symmetrization scheme in real space[35] utlizing the HEG-like renormalized adiabatic LDA (rALDA) kernel.[32]

Within this approach, a general MGGA xc-kernel is represented in reciprocal space as

$$f_{\mathrm{xc}}^{\mathbf{G}\mathbf{G}'}(\mathbf{q};\omega) = \frac{1}{\Omega}\int_{\Omega} d\mathbf{r}\, e^{-i(\mathbf{G}-\mathbf{G}')\cdot\mathbf{r}} \times f_{\mathrm{xc}}[n(\mathbf{r}),\tau(\mathbf{r})](\sqrt{|\mathbf{q}+\mathbf{G}||\mathbf{q}+\mathbf{G}'|};\omega)\,, \tag{15}$$

where Ω is the unit-cell volume. Since construction of each matrix element of the kernel via Fast Fourier Transform (FFT) is independent, we parallelize the construction of f_{xc} by distributing the rows of the matrix such that each core performs approximately the same number of FFTs. Since the kernel is Hermitian, we can also reduce the expense by computing the corresponding triangular matrix. After constructing the kernel in reciprocal space, the infinite-order response function is constructed by inverting the dielectric matrix

$$\epsilon_\lambda(\mathbf{q};iu) = 1-\chi_0(\mathbf{q};iu)\left[V_\lambda(\mathbf{q})+f_{\mathrm{xc}}^{\lambda}(\mathbf{q};iu)\right], \tag{16}$$

obtaining the interacting response function as $\chi_\lambda(\mathbf{q};iu) = \epsilon_\lambda^{-1}(\mathbf{q};iu)\chi_0(\mathbf{q};iu)$, and the correlation energy from Eq. (3).

For the renormalized methods using exchange-like kernels, the coupling-strength integration can be done analytically for RPAr1 and ACSOSEX. Introducing the Hermitian matrices $Q = V^{\frac{1}{2}}\chi_0 V^{\frac{1}{2}}$, $\tilde{Q}=1-Q$, and transformed kernel $\tilde{f}_{\mathrm{x}} = V^{-\frac{1}{2}} f_{\mathrm{x}} V^{-\frac{1}{2}}$, the resulting bRPA correlation energies are

$$\Delta E_c^{\mathrm{RPAr1}}[f_{\mathrm{x}}] = -\frac{1}{2\pi}\sum_{\mathbf{q}}\int_0^\infty du\, \Big\langle \tilde{f}_{\mathrm{x}}(\mathbf{q};iu) \times\Big[\Big[\tilde{Q}(\mathbf{q};iu)\Big]^{-1}Q(\mathbf{q};iu) -\ln\Big[\tilde{Q}(\mathbf{q};iu)\Big]\Big]\Big\rangle, \tag{17a}$$

$$\Delta E_c^{\mathrm{ACSOSEX}}[f_{\mathrm{x}}] = -\frac{1}{2\pi}\sum_{\mathbf{q}}\int_0^\infty du\, \Big\langle \tilde{f}_{\mathrm{x}}(\mathbf{q};iu) \times\Big[Q(\mathbf{q};iu)-\ln\Big[\tilde{Q}(\mathbf{q};iu)\Big]\Big]\Big\rangle. \tag{17b}$$

Once the kernel has been computed, RPA, RPAr1, and ACSOSEX correlation energies can be computed simultaneously since they can all be expressed as functions of the matrix Q. The coupling strength integral can be performed analytically for the infinite-order method[11,29], however an inversion of χ_0 is required which may become numerically unstable at certain frequencies.[32] We stress that since ACSOSEX and RPAr1 have analytic λ-integrations with exchange-like kernels, and only the matrix Q must be diagonalized, the additional expense of a numerical coupling strength integration or inversion of χ_0 required for the infinite-order method compared to RPA is entirely avoided. Thus given an efficient algorithm to compute χ_0[55] and one for the kernel, there is no major increase in expense compared to RPA to evaluate the ACSOSEX and RPAr1 corrections.

In order to avoid numerical issues related to the $\mathbf{q}\to 0$ limit of the Coulomb interaction we neglect the contributions from the head and wings at the Γ-point.[56] As discussed in Ref. 56, including these contributions in the evaluation of the EXX and correlation energies can cause kinks in the energy-volume curves and slows the convergence with respect to the k-point sampling, but does not alter the converged results. Since we converged the EXX and correlation energies separately for each system we also expect this approximation to have a negligible impact on the final results. We have implemented the working equations above into a modified version of the ABINIT software,[57] which was used for the calculations of inhomogenous systems. Results for the homogeneous electron gas (HEG) have been computed with an independent FORTRAN code.

V. RESULTS

In order to distinguish between the various methods introduced above we use the following nomenclature: the kernel name alone will refer to the infinite-order method for χ_λ, Eq. (10), RPAr1 to Eq. (13), and ACSOSEX to Eq. (14), each evaluated with the NEO kernel. When one method is used but with different values of $\tilde{c}$, the value of the parameter is appended to the name of the method.

A. Homogeneous Electron Gas

The NEO correlation energy for the spin-unpolarized HEG as a function of $\tilde{c}$ and the Seitz radius, $r_s = (3/4\pi n)^{1/3}$, is illustrated in Fig. 1. The dashed, vertical line indicates $\tilde{c} = 0.264$ which is the value determined by the constraint on the second-order exchange energy, Eq. (9). For r_s between 1 and 20, $\tilde{c} = 0.264$ produces a

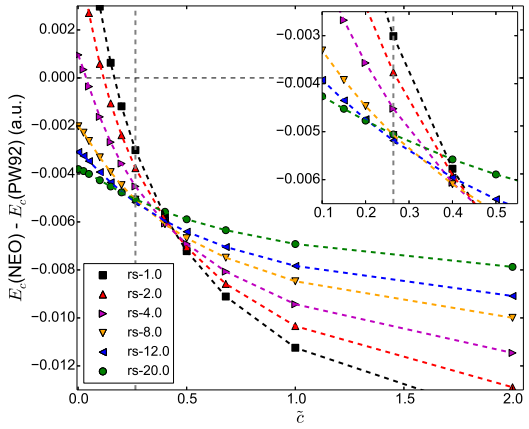

FIG. 1. Variation of the total correlation energy difference $E_c(\text{NEO}) - E_c(\text{PW92})$ with respect to changes in $\tilde{c}$. The vertical, dashed line indicates $\tilde{c} = 0.264$. Compared to the constrained value, $\tilde{c} = 0.4$ yields a smaller distribution of errors, but a larger absolute error. The inset shows an enhanced view for $\tilde{c}$ between 0.1 and 0.5.

distribution of errors compared to PW92[58] between approximately 3 and 5 mH, with the error increasing until about $r_s = 12$ whereafter it remains essentially constant. The width of the error distribution is approximately 2 mH and the error for all r_s is systematically an underestimate.

Increasing $\tilde{c}$ to 0.4 results in a narrower distribution of errors, approximately 0.5 mH in width for $1 \leq r_s \leq 20$, but increases the error for all r_s in comparison to $\tilde{c} = 0.264$. Beyond $\tilde{c} = 0.4$ the errors in the low-density regime become smaller than those in the high-density regime and the difference in errors grows as well; by $\tilde{c} = 1$ the width of the distribution of errors is nearly 5 mH. Decreasing $\tilde{c}$ below 0.264 leads to smaller errors for the high-density limit, but the error distribution width becomes much larger (almost 15 mH for $\tilde{c} \approx 0$). Moreover, for $\tilde{c}$ less than approximately 0.2, NEO is no longer a systematic underestimate for smaller values of r_s. Thus we find the constraint on $\tilde{c}$ through Eq. (9) to be useful for the HEG since it produces a kernel that delivers errors of approximately 4 ± 1 mH over a wide range of densities and is a systematic underestimate with respect to the exact result. Further support for this conclusion can be found by analyzing the q-dependence of the correlation energy.

The wave-vector decomposition[40] of the total and bRPA correlation energy per particle at $r_s = 4$ for NEO with three particular values of $\tilde{c}$, RPA, and the exact curve are shown in Fig. 2. The total correlation energy plot implies that NEO decays too quickly for larger q and does not fully cancel RPA, while the agreement for small to intermediate q can be tuned by changing $\tilde{c}$. For spin-unpolarized systems, in the limit $q \to \infty$, $f_{\text{x}}^{\text{NEO}}(q) \approx -V(q)/2$, which is essentially a factor of two too small. There is a price for the improved agreement of the wave-vector decomposition, however, since as $\tilde{c}$ increases so does the magnitude of the correlation energy (the integral of $\epsilon_c(q)$). For $r_s = 4$ the integrated errors of the NEO correlation energy compared to PW92 are 20 μH, 1.6 mH, and 2.2 mH for $\tilde{c} = 0.0375$, 0.264, and 0.4, respectively.

Looking at the bRPA contribution, the rapid decay of the NEO correction for larger q is explicitly demonstrated. The smallest value of $\tilde{c}$ mimics the overall shape and area of the exact curve, but contributions at small q are largely overestimated. For $\tilde{c} = 0.264$ and 0.4 the agreement with the exact curve is greatly improved for small q, but the maximum contribution is underestimated. Since $\tilde{c} = 0.264$ provides a balance in the cancellation of errors of the wave-vector decomposition for small and large q and the total integrated error compared to PW92 we find the second-order exchange constraint sufficient to determine the value of $\tilde{c}$.

B. RPA Renormalization for the Electron Gas

Rather than empirically tuning $\tilde{c}$ to adjust the range of the kernel, the contributions to the wave-vector decomposition and subsequently to the total correlation energy can be naturally modulated through approximations for χ_λ. Using the constrained value of $\tilde{c}$, ACSOSEX and RPAr1 were computed in combination with the NEO kernel and the errors compared to PW92 for the correlation energy per particle are shown in Fig. 3. ACSOSEX performs quite well, lowering the error compared to NEO by 2.5 mH on average, whereas RPAr1 increases the error compared to NEO by approximately 0.6 mH. The good performance of ACSOSEX is somewhat surprising since it is a method intended to be accurate for one- and two-electron like systems, so why does it perform so well?

Plots of the beyond-RPA contributions to the correlation energy, Eq. (12) and Eq. (17), are shown in Fig. 4. ACSOSEX, RPAr1, and NEO all contain some level of long-range screening due to the different re-summations (replacing χ_0 with $\hat{\chi}_\lambda$ or χ_λ in Eq. (9)), so the small q behavior is naturally modulated by the approximations for the response function. The short-ranged (large q) behavior is, however, dominated by the behavior of the kernel since all three methods approach the same value in the tail of $\Delta\epsilon_c(q)$.

Apart from a rigid shift to smaller q, the ACSOSEX curve mimics the exact curve in both the maximum contribution and overall shape. Much like changing $\tilde{c}$ to

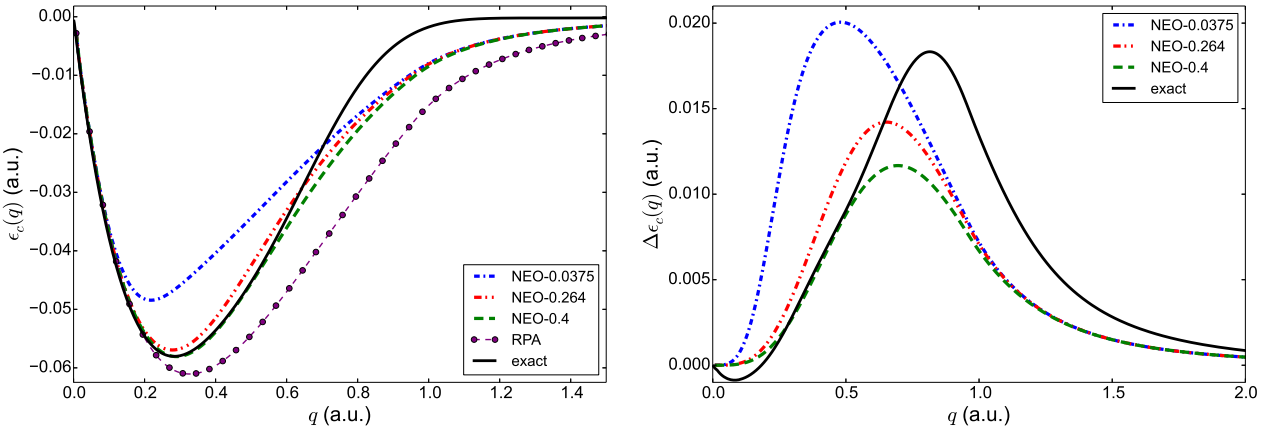

FIG. 2. Wave-vector decomposition of the total (left) and bRPA (right) correlation energy per particle, Eqs. (4) and (12), for the spin-unpolarized HEG at $r_s = 4$. The "exact" curve is the Fourier transform of the pair-density model of Ref 59.[60] The small, negative region of the exact bRPA curve is most likely an artifact of the fitting procedures used to construct the real space pair-density model. Increasing the value of $\tilde{c}$ to 0.4 improves the agreement of NEO with the exact curve for small to moderate q, but leads to a larger integrated error.

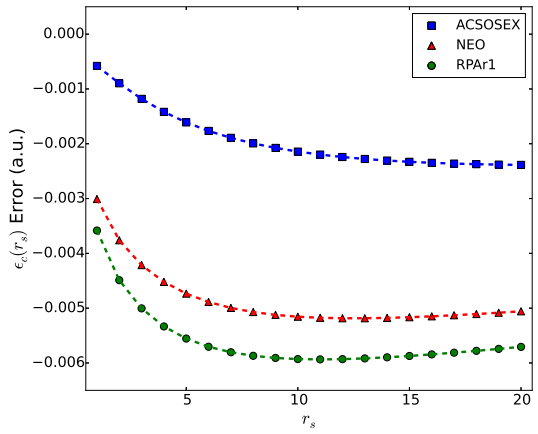

FIG. 3. The error, $\epsilon_c(\text{Method}) - \epsilon_c(\text{PW92})$, as a function of r_s for $\tilde{c} = 0.264$. ACSOSEX yields a systematic overestimate of the NEO correction, while RPAr1 a systematic underestimate.

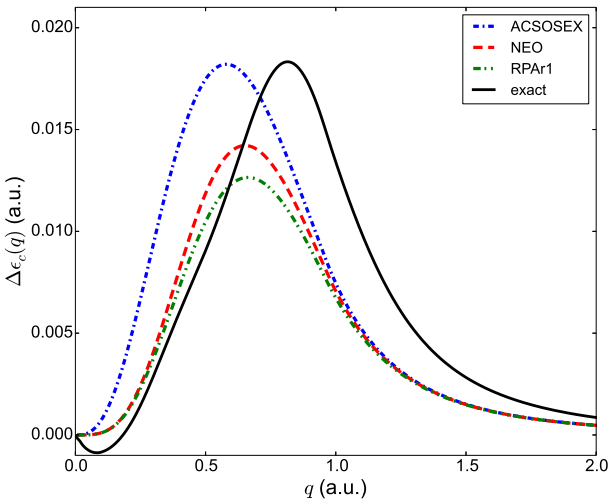

FIG. 4. Beyond RPA correlation energy per particle for $r_s = 4$ using three different approximations for χ_λ. For a fixed $\tilde{c}$, ACSOSEX mimics the impact of decreasing $\tilde{c}$ on the infinite-order method, while RPAr1 mimics the behavior of increasing $\tilde{c}$.

smaller values for the infinite-order NEO method, ACSOSEX benefits from the cancellation of errors that for smaller q the bRPA correction is an overestimate, but for larger q an underestimate compared to the exact curve. The additional screening in RPAr1 and NEO compared to ACSOSEX reduces the error for small q, but the maximum contribution is simultaneously reduced. Thus ACSOSEX, with the replacement $\chi_\lambda \to \chi_0$ in Eq. (12), combined with the NEO kernel yields a balance of nonlocality and screening in the electron gas that results in an accurate method due to cancellation of errors.

In essence the renormalized approaches are limited in their accuracy by the infinite-order method. For kernels which overestimate the bRPA correction in comparison to some exact reference, RPAr1 would reduce the error while ACSOSEX would exaggerate it, and *vice versa* for kernels which underestimate compared to an exact reference. The good fortune of ACSOSEX-NEO for the HEG is not general, and we demonstrate this for non-metallic inhomogeneous systems where RPAr1-NEO yields superior results.

C. RPA Renormalization for Inhomogeneous Systems

The lattice constants and bulk moduli of diamond C and Si, zinc blende AlN, and fcc Al were computed using both a PBE[61] and LDA based Troullier-Martins norm-conserving (NC) pseudopotential[62], and the results are gathered in Tables II and III. We include the results from Ref. 35 for rALDAx, another exchange-like kernel[32], for comparison. Large cutoff energies and tight convergence parameters were used to avoid excessive testing, and these parameters have been gathered in the supporting information.[63] The correlation energies were extrapolated using two cutoffs according to the Harl-Kresse procedure,[16,56] except for Al where we used a convergent cutoff. Shifted $n \times n \times n$ Monkhorst-Pack k-meshes with $n = 4$ were used for the correlation energy and at least $n = 6$ for the EXX energy. We found the differences in non-metallic structural properties for $n = 4$ and $n = 2$ for the PBE reference to be negligible (see supporting information) so only $n = 2$ meshes were used to compute the ACFD@LDA results for C, Si, and AlN. At least six volume points close to the minimum were used to fit the Birch-Murnaghan equation of state for each system.

	a_0 (Å)	RPA	ACSOSEX	RPAr1	NEO
HEG	$r_s = 2$	–0.06180	–0.04566	–0.04925	–0.04852
C (A4)	3.595	–0.52210	–0.34984	–0.38796	–0.37497
Si (A4)	5.420	–0.44858	–0.29370	–0.32886	–0.31622
AlN (B3)	4.376	–0.49587	–0.28471	–0.33543	–0.31974
Al (A1)	4.053	–0.18179	–0.13138	–0.14324	–0.14064

TABLE I. Extrapolated total correlation energies (a.u.) for C, Si, AlN, and Al using a PBE reference, and correlation energy per particle for the HEG. The structure is indicated in parenthases. The three kernel corrected methods were all evaluated with the NEO kernel using $\tilde{c} = 0.264$. RPAr1 underestimates the NEO correlation energy by 2-5%.

Before discussing the structural properties it is useful to analyze the trends in total correlation energies. The correlation energies for PBE based RPA and the three NEO-based methods for a fixed volume are given in Table I. ACSOSEX-NEO is approximately 6-11% more positive and RPAr1-NEO 2-5% more negative than NEO for the systems studied here. The relative magnitudes of ACSOSEX and RPAr1 for the HEG at $r_s = 2$ are quite close to those for Al ($r_s = 2.07$), indicating these low-order RPA renormalized methods are robust perturbation theories for model and real metallic systems. This is particularly remarkable since traditional low-order many-body perturbation theory diverges for metals.[37,64–66] The fact that the first order in RPA renormalization recovers at least 95% of the infinite-order result is indicative of a rapidly converging perturbative expansion, but this remains to be proven in general. Unpublished tests with other model kernels for the HEG show this relative performance persists regardless of the choice in kernel implying this is truly a feature of the method.

The consistent behavior of the renormalized methods directly translates to shifted structural properties in comparison to the infinite-order NEO results. Based on the PBE reference results in Table II, the NEO kernel does improve upon the already accurate RPA by maintaining the 0.01 Å deviation of the lattice constants and slightly reducing the errors for the bulk moduli. The lattice constants are subsequently shorter and bulk moduli larger for ACSOSEX compared to NEO because the bRPA correction is overestimated, while for RPAr1 a_0 and B are larger and smaller than NEO because the correction is underestimated. ACSOSEX-NEO appeared to be a promising method based on the smaller errors in the HEG correlation energies, but RPAr1-NEO leads to smaller errors for structural properties compared to both experiment and the infinite-order method for the non-metallic cases. For aluminum all three methods yield essentially equivalent results. NEO with a PBE reference appears to perform slightly better compared to experiment than rALDAx with an LDA reference, but given the dependence on the reference discussed below we hesitate to make any direct, in-depth comparisons.

D. Pseudopotential and Reference Dependence

While some aspects of the ACFD results are sensitive to the reference, others are typically insensitive. For C, Si, and AlN with either reference, addition of the kernel tends to reduce the lattice constant and increase the bulk modulus in comparison to RPA. This is somewhat expected since RPA is known to underbind, so adding a kernel correction should increase the bond strength and reduce the lattice constant.[49] In Al, however, addition of the NEO kernel to RPA increases the lattice constant and decreases the bulk modulus. This trend for Al was also seen for a number of other kernels in Ref 35. The relative magnitudes of the kernel corrections discussed in Table I were also found to be insensitive to the reference. Unfortunately the structural properties show a direct dependence on the reference.

The PBE based ACFD results (Table II) generally show small errors in comparison to experiment, but error cancellation plays a role since using an LDA reference leads to an entirely different trend, Table III. We use the notation Method@DFT to indicate the reference used to evaluate the Method energy. The difference in our results for a given method with each reference stems primarily from the differences in the EXX total energies. Evidence of this behavior was obscured previously as the NC RPA@LDA results of Ref 34 differ noticeably from the PAW results of Refs 35 and 56 for silicon, but the EXX results were not always explicitly discussed. In fact our RPA@LDA result for Si is in good agreement with that of Ref. 34 indicating the similar performance of our pseudopotentials for EXX@LDA. In contrast, the PAW-based RPA structures obtained with a PBE or LDA reference

for C, Si, and Cu reported in Ref 56 do not show a large difference since the EXX properties are equivalent and the impact of correlation is the same for both references. ACFD atomization energies for small molecules have also been evaluated with PAW or Gaussian basis set implementations using different references and the EXX contributions reported to be insensitive to the reference.[32,38] The discrepancy in our results is likely due to the difficulty of capturing the fully non-local EXX energy and core-valence interaction[67–70] with a simple NC pseudopotential that has been parametrized for a semi-local functional.

Such a dependence on the reference and NC pseudopotential complicates the comparison of structural properties to experiment for ACFD methods as the accuracy will be limited by that of EXX@DFT. The RPA results we obtained with a PBE reference show much better agreement with experiment than those obtained with the LDA reference for precisely this reason; the errors of EXX@PBE are reduced by addition of RPA correlation, while the errors of EXX@LDA are too large to be overcome by the addition of correlation. In fact RPA@LDA yields larger errors than EXX@LDA and addition of the kernel yields even larger errors. Thus the performance of a kernel corrected method depends to some extent on the error cancellation between EXX and RPA. If the RPA error compared to experiment is due to its underbinding then addition of a kernel correction should reduce the errors, but if the major source of error compared to experiment stems from the performance of EXX@DFT, then adding a kernel correction can exaggerate the errors further as seen in Table III.

VI. CONCLUSION

We have introduced a non-local, energy optimized, exchange-like kernel that is constrained to recover the exact second-order exchange correlation energy of the homogeneous electron gas. Based on a PBE reference, the NEO kernel produces accurate structural properties for the inhomogeneous systems we tested compared to experiment, reducing the underbinding of RPA. RPA renormalization was also explored for solids in the form of the ACSOSEX and RPAr1 approximations for the response function. Both approaches produce systematic correlation energies that over and underestimate, respectively, the infinite-order method, but do not significantly increase the computational cost in comparison to RPA for exchange-like kernels. Furthermore, these methods are robust perturbation theories that can be directly applied to metallic systems, eliminating the divergence for zero-gap systems of standard perturbative approaches. The impact of the reference and norm-conserving pseudopotential on ACFD structural properties was also explored and found to play a large role in comparisons of the results to experiment.

ACKNOWLEDGEMENTS

We thank F. Bruneval, J. P. Perdew and F. Furche for useful discussions. This work was supported by the Department of Energy under Grant No. DE–SC0010499, and in part by the National Science Foundation through major research instrumentation Grant No. CNS–09–58854. This project was partially completed using resources from the National Energy Research Scientific Computing Center (NERSC) under Award Nos. DE–SC0012575 and DE–SC0010499. Figures were created using MATPLOTLIB[71].

* Electronic mail: jeb@temple.edu
† Current address: Department of Physics, King's College London, London WC2R 2LS, United Kingdom

[1] P. Hohenberg and W. Kohn, Phys. Rev. **136**, B864 (1964).
[2] W. Kohn and L. J. Sham, Phys. Rev. **140**, A1133 (1965).
[3] R. M. Dreizler and E. K. U. Gross, eds., *Densty Functional Theory* (Springer, 1990).
[4] W. Kohn, A. D. Becke, and R. G. Parr, J. Phys. Chem. **100**, 12974 (1996).
[5] C. Fiolhais, F. Nogueira, and M. Marqués, eds., *A Primer in Density Functional Theory* (Springer, 2003).
[6] J. P. Perdew and A. Zunger, Phys. Rev. B **23**, 5048 (1981).
[7] P. Mori-Sánchez, A. J. Cohen, and W. Yang, Phys. Rev. A **85**, 042507 (2012).
[8] Y. Andersson, D. C. Langreth, and B. I. Lundqvist, Phys. Rev. Lett. **76**, 102 (1996).
[9] J. P. Perdew, R. G. Parr, M. Levy, and J. L. Balduz, Phys. Rev. Lett. **49**, 1691 (1982).
[10] P. Nozières and D. Pines, Phys. Rev. **85**, 338 (1952).
[11] D. C. Langreth and J. P. Perdew, Phys. Rev. B **15**, 2884 (1977).
[12] H. Eshuis, J. E. Bates, and F. Furche, Theor. Chem. Acc. **131**, 1084 (2012).
[13] J. P. Perdew and K. Schmidt, in *Density Functional Theory and Its Application to Materials*, Vol. 577, edited by V. Van Doren, C. Van Alsenoy, and P. Geerlings (AIP, 2001) pp. 1–20.
[14] J. F. Dobson and J. Wang, Phys. Rev. Lett. **82**, 2123 (1999).
[15] J. F. Dobson, J. Wang, B. P. Dinte, K. McLennan, and H. M. Le, Int. J. Quantum Chem. **101**, 579 (2005).
[16] J. Harl and G. Kresse, Phys. Rev. B **77**, 045136 (2008).
[17] S. Lebègue, J. Harl, T. Gould, J. G. Ángyán, G. Kresse, and J. F. Dobson, Phys. Rev. Lett. **105**, 196401 (2010).
[18] H.-V. Nguyen and G. Galli, J. Chem. Phys. **132**, 044109 (2010).

[19] H. Eshuis and F. Furche, J. Phys. Chem. Lett. **2**, 983 (2011).
[20] F. Furche and T. Van Voorhis, J. Chem. Phys. **122**, 164106 (2005).
[21] F. Furche, Phys. Rev. B **64**, 195120 (2001).
[22] Z. Yan, J. P. Perdew, and S. Kurth, Phys. Rev. B **61**, 16430 (2000).
[23] A. Ruzsinszky, J. P. Perdew, and G. I. Csonka, J. Chem. Theory Comput. **6**, 127 (2010).
[24] B. Xiao, J. Sun, A. Ruzsinszky, J. Feng, and J. P. Perdew, Phys. Rev. B **86**, 094109 (2012).
[25] D. Bohm and D. Pines, Phys. Rev. **85**, 338 (1952).
[26] H. Jiang and E. Engel, J. Chem. Phys. **127**, 184108 (2007).
[27] J. Paier, X. Ren, P. Rinke, G. Scuseria, A. Grüneis, G. Kresse, and M. Scheffler, New. J. of Phys. **14**, 043002 (2012).
[28] A. Hesselmann and A. Görling, Phys. Rev. Lett. **106**, 093001 (2011).
[29] N. Colonna, M. Hellgren, and S. de Gironcoli, Phys. Rev. B **90**, 125150 (2014).
[30] M. Corradini, R. Del Sole, G. Onida, and M. Palummo, Phys. Rev. B **57**, 14569 (1998).
[31] L. A. Constantin and J. M. Pitarke, Phys. Rev. B **75**, 245127 (2007).
[32] T. Olsen and K. S. Thygesen, Phys. Rev. B **86**, 081103(R) (2012).
[33] P. E. Trevisanutto, A. Terentjevs, L. A. Constantin, V. Olevano, and F. D. Sala, Phys. Rev. B **87**, 205143 (2013).
[34] D. Lu, J. Chem. Phys. **140**, 18A520 (2014).
[35] C. E. Patrick and K. S. Thygesen, J. Chem. Phys. **143**, 102802 (2015).
[36] J. F. Dobson and J. Wang, Phys. Rev. B **62**, 10038 (2000).
[37] A. Grüneis, M. Marsman, and G. Kresse, J. Chem. Phys. **133**, 074107 (2010).
[38] J. E. Bates and F. Furche, J. Chem. Phys. **139**, 171103 (2013).
[39] M. Petersilka, U. J. Gossmann, and E. K. U. Gross, Phys. Rev. Lett. **76**, 1212 (1996).
[40] M. Lein, E. K. U. Gross, and J. P. Perdew, Phys. Rev. B **61**, 13431 (2000).
[41] J. Tao, J. P. Perdew, V. N. Staroverov, and G. E. Scuseria, Phys. Rev. Lett. **91**, 146401 (2003).
[42] J. P. Perdew, A. Ruzsinszky, G. I. Csonka, L. A. Constantin, and J. Sun, Phys. Rev. Lett. **103**, 026403 (2009).
[43] J. Jung, P. García-González, J. F. Dobson, and R. W. Godby, Phys. Rev. B **70**, 205107 (2004).
[44] L. Onsager, L. Mittag, and M. J. Stephen, Ann. Phys. (Leipzig) **18**, 71 (1966).
[45] U. von Barth and L. Hedin, J. Phys. C **5**, 1629 (1972).
[46] D. C. Langreth and J. P. Perdew, Solid State Commun. **17**, 1425 (1975).
[47] G. Jansen, R.-F. Liu, and J. G. Ángyán, J. Chem. Phys. **133**, 154106 (2010).
[48] D. L. Freeman, Phys. Rev. B **15**, 5512 (1977).
[49] A. Grüneis, M. Marsman, J. Harl, L. Schimka, and G. Kresse, J. Chem. Phys. **131**, 154115 (2009).
[50] B. T. Krull and F. Furche, unpublished.
[51] J. Jung, P. Garćia-Gonźalez, J. F. Dobson, and R. W. Godby, Phys. Rev. B **70**, 205107 (2004).
[52] T. Olsen and K. S. Thygesen, Phys. Rev. B **88**, 115131 (2013).
[53] P. Ghosez, X. Gonze, and R. W. Godby, Phys. Rev. B **56**, 12811 (1997).
[54] W. G. Aulbur, L. Jönsson, and J. W. Wilkins, Phys. Rev. B **54**, 8540 (1996).
[55] M. Kaltak, J. Klimeš, and G. Kresse, Phys. Rev. B **90**, 054115 (2014).
[56] J. Harl, L. Schimka, and G. Kresse, Phys. Rev. B **81**, 115126 (2010).
[57] X. Gonze and et al., Computer Phys. Comm. **180**, 2582 (2009); available at `http://www.abinit.org`
[58] J. P. Perdew and Y. Wang, Phys. Rev. B **45**, 13244 (1992).
[59] P. Gori-Giorgi and J. P. Perdew, Phys. Rev. B **66**, 165118 (2002).
[60] The original code for the pair-density model is graciously provided by the author at `http://www.paolagorigiorgi.org`.
[61] J. P. Perdew, K. Burke, and M. Ernzerhof, Phys. Rev. Lett. **77**, 3865 (1996).
[62] FHI Troulliler-Martins NC pseudopotentials, `http://www.abinit.org/downloads/psp-links/`, accessed: 09-01-2015.
[63] See Supplemental Material at [URL will be inserted by publisher] for full summaries of data and parameters used for each system.
[64] A. L. Fetter and J. D. Walecka, *Quantum Theory of Many-Particle Systems* (Dover, 2003).
[65] J. J. Shepherd and A. Grüneis, Phys. Rev. Lett. **110**, 226401 (2013).
[66] J. J. Shepherd, T. M. Henderson, and G. E. Scuseria, J. Chem. Phys. **140**, 124102 (2014).
[67] M. Fuchs, M. Bockstedte, E. Pehlke, and M. Scheffler, Phys. Rev. B **57**, 2134 (1998).
[68] E. Engel, A. Höck, R. N. Schmid, R. M. Dreizler, and N. Chetty, Phys. Rev. B **64**, 125111 (2001).
[69] S. Sharma, J. K. Dewhurst, and C. Ambrosch-Draxl, Phys. Rev. Lett. **95**, 136402 (2005).
[70] J. R. Trail and R. J. Needs, J. Chem. Phys. **122**, 014112 (2005).
[71] J. D. Hunter, Comput. Sci. Eng. **9**, 90 (2007).

		PBE	EXX	EXX[a]	RPA	RPA[a]	ACSOSEX-NEO	RPAr1-NEO	NEO	Expt
C	a_0	3.561	3.546	3.540	3.573	3.572	3.546	3.568	3.560	3.553
	B	433	494	512	425	441	457	432	440	443
Si	a_0	5.455	5.474	5.482	5.413	5.432	5.399	5.417	5.406	5.421
	B	90	106	108	96	99	104	98	100	99
AlN	a_0	4.396	4.346	4.346	4.384	4.394	4.345	4.379	4.370	4.368
	B	188	232	240	206	200	219	204	207	202
Al	a_0	4.046	4.094	4.104	4.022	4.037	4.037	4.043	4.042	4.018
	B	76	64	61	74	77	72	70	71	79
MD	a_0	0.025	0.025	0.028	0.008	0.019	–0.008	0.012	0.004	
	B	–9	18	24	–6	–2	7	–5	–1	
MAD	a_0	0.025	0.040	0.046	0.012	0.019	0.018	0.014	0.012	
	B	9	26	34	8	2	11	6	4	

[a] PAW PBE reference results from Ref. 56

TABLE II. PBE reference results for each method. MD and MAD are the mean deviation and mean absolute deviation with respect to experiment. The EXX@PBE a_0 and B are typically larger than the experiment so that addition of ACFD correlation reduces the error. ACSOSEX-NEO and RPAr1-NEO are systematically an overestimate and an underestimate, respectively, in comparison to NEO for the magnitude of the bRPA correction. Corrected experimental values for a_0, but not for B, were taken from Ref 56 and references therein. The lattice constants are reported in Å and the bulk moduli in GPa.

		LDA	EXX	RPA	RPA[a]	ACSOSEX-NEO	RPAr1-NEO	NEO	rALDAx[b]
C	a_0	3.518	3.515	3.537	3.566	3.518	3.534	3.526	3.563
	B	466	512	435	435	483	447	459	435
Si	a_0	5.380	5.405	5.345	5.449	5.333	5.350	5.340	5.456
	B	96	111	106	95	111	106	108	95
AlN	a_0	4.302	4.261	4.258	–	4.219	4.252	4.244	–
	B	208	244	208	–	231	212	216	–
Al	a_0	3.962	3.999	3.931	4.042	3.946	3.951	3.95	4.053
	B	84	78	85	78	83	81	82	78
MD	a_0	–0.050	–0.045	–0.072	0.022	–0.086	–0.068	–0.075	0.027
	B	8	31	3	–4	21	6	11	–4
MAD	a_0	0.050	0.045	0.072	0.022	0.086	0.068	0.075	0.027
	B	9	31	7	4	21	6	11	4

[a] PAW RPA@LDA from Ref. 35
[b] PAW rALDAx@LDA from Ref. 35

TABLE III. LDA reference results for each method. MD and MAD are the mean deviation and mean absolute deviation with respect to experiment. The EXX@LDA lattice constants are already too small compared to experiment, and as a result the correlated methods largely underestimate a_0. The bulk moduli are simultaneously overestimated. The lattice constants are reported in Å and the bulk moduli in GPa.